Finite-Element Modeling and Modal Analysis of an Actuated Platform used for Precision Pointing Control

Gerardo Zarate, Eric Diaz, Jessica Alvarenga, Khosrow Rad and Helen Boussalis, *Member, IEEE*

***Abstract*— A large, segmented space telescope requires high precision and accuracy in its mirror shape to obtain clear images. The SPACE Telescope Testbed at the Structures, Propulsion, and Control Engineering (SPACE) Laboratory must maintain a pointing control accuracy of 2 arc seconds. A Peripheral Pointing Architecture (PPA) has been designed to demonstrate the telescope pointing accuracy. A finite element model of the PPA is developed using FEMAP. Modal analysis is performed on the finite element model resulting in the natural frequencies, mode shapes, eigenvalues, mass matrix, stiffness matrix, and degree of freedom mapping of the PPA structure.**

I. Introduction

Due to an ever increasing need to see further into space, the successor to the Hubble Space Telescope (HST) is required. Younger objects, receding from us at an ever-faster rate, are red-shifted into the near infrared where Hubble loses sensitivity.

To meet the requirement of the National Aeronautics and Space Administration (NASA) for future telescopes, the new infrared (IR) space observatory will replace the Hubble Space Telescope after the end of its useful life. Serving as the successor to the HST, the James Webb Space Telescope (JWST), previously known as the Next Generation Space Telescope (NGST), requires a larger light-gathering primary mirror capable of detecting faint signals from the first billion years, the period when galaxies formed. The JWST will be capable of detecting radiation whose wavelength lies in the range of 0.6 to 20 mm (and be optimized for the 1 to 5 mm region). Furthermore, the JWST must be able to see objects 400 times fainter than those currently studied with large ground-based infrared telescopes such as the Keck Observatory.

Due to the size and weight limitations associated with current launch vehicles, future missions, such as the JWST, will employ segmented reflectors, rather than monolithic reflectors cast from a single piece of glass. Although multiple-mirror designs have many advantages, a number of major difficulties are associated with this technique. The mirrors can be easily misaligned due to disturbances; therefore a controller is necessary for maintenance of mirror shape. Another challenge in the integration of such advanced optical systems is the stringent requirements for the pointing of the telescope.

To study the control of such large segmented optical systems, the NASA in 1994 provided funding to establish the Structures, Propulsion and Control Engineering (SPACE) Laboratory at California State University, Los Angeles (CSULA). One of the major goals of this project is to design and fabricate a Testbed that resembles the complex dynamic behavior of a segmented space telescope. The SPACE Testbed being a control oriented structure mostly investigates the control challenges of figure maintenance and precision pointing.

The SPACE Testbed together with an actuated laser platform allows for demonstration of precision pointing control and figure maintenance. The actuated laser platform is modeled using finite element techniques in order to extract the necessary modal parameters needed to develop a state space model. This model will be used in controller design that will achieve both shaping and pointing accuracy as required by NASA.

II. The SPACE Testbed Description

The SPACE Testbed shown in Figure 1 emulates a Cassegrain telescope of 2.4-meter focal length with performance comparable to an actual space-borne system. The system's top-level requirements include figure maintenance of the primary mirror to within 1 micron RMS distortion with respect to a nominal shape of the primary mirror, and precision pointing with accuracy of 2 arc seconds.

Manuscript received January 29, 2012. This work was supported in part by NASA under Grand URC NNX08B44A.

G. Zarate is with the Electrical Engineering Department, California State University, Los Angeles, LA, CA 90032 USA, (phone: 323-343-5445; e-mail: gzarate@calstatela.edu).

E. Diaz is with the Electrical Engineering Department, California State University, Los Angeles, LA, CA 90032 USA, (e-mail: ediaz6@calstatela.edu).

J. Alvarenga is with the Electrical Engineering Department, California State University, Los Angeles, LA, CA 90032 USA, (e-mail: jalvare5@calstatela.edu).

K. Rad is with the Electrical Engineering Department, California State University, Los Angeles, LA, CA 90032 USA, (e-mail: krad@calstatela.edu).

H. Boussalis is with the Electrical Engineering Department, California State University, Los Angeles, LA, CA 90032 USA, (e-mail: hboussa@calstatela.edu).

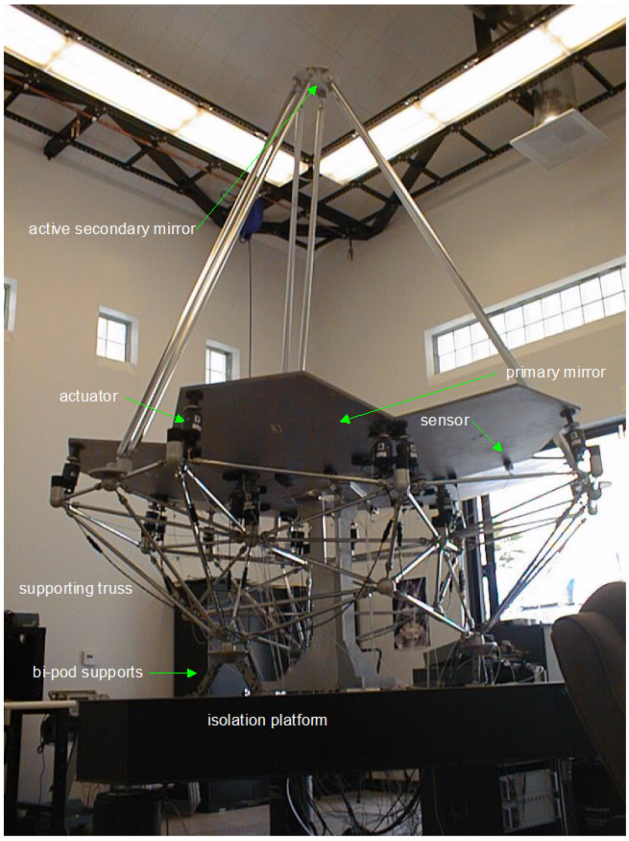

Figure 1. SPACE Testbed

The SPACE Testbed consists of a primary mirror, a secondary mirror and a lightweight flexible truss structure. The primary mirror (mounted on the support truss) consists of seven hexagonal panels, each 101 cm in diameter. The six peripheral panels are actively controlled in the three degrees-of-freedom by 18 linear electromagnetic actuators (3 actuators per active panel), and the seventh panel is used as a reference. In addition, a set of 18 edge sensors are used to provide measurements of relative displacement and angle of the panels (3 sensors per active panel). The Testbed's active secondary mirror is a six-sided pyramidal mirror used to reflect the light from the primary mirror to the central plane and is attached to the primary by a tripod. The entire Testbed is supported by a triangular isolation platform made of aluminum honeycomb core with stainless steel top and bottom skin.

III. Peripheral Pointing Architecture

The SPACE Telescope Testbed is required to perform precision pointing while maintaining the parabolic shape of the primary mirror. In order to achieve pointing control of the Testbed accurate to 2 arc seconds, a Peripheral Pointing Architecture (PPA) has been designed to physically demonstrate telescope pointing by simulating light rays from distant objects, Figure 2. The PPA structure is shown in Figure 3.

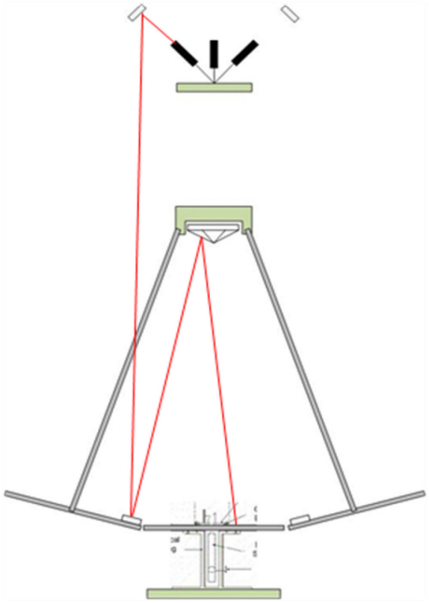
Figure 2. SPACE Testbed PPA Laser Path

The PPA uses an assembly of six lasers as shown in Figure 4 to simulate the object of study. Each laser corresponds to its own separate panel and optical detector. The laser assembly sits on a motorized tip/tilt platform and the laser source coincides with the rotation, or gimbal, point of the platform.

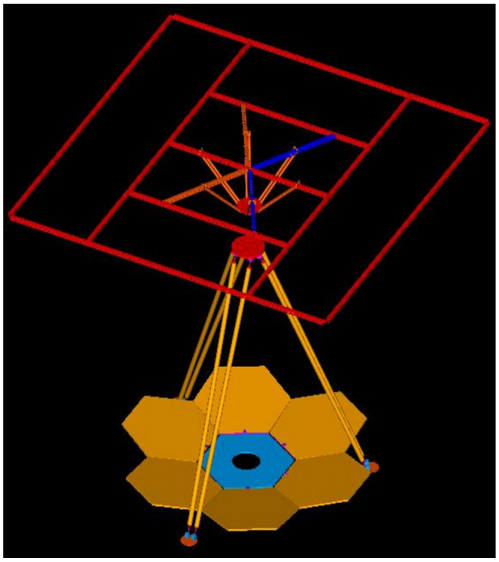
Figure 3. PPA Structure

Since the laser source lies on the rotation point of the platform, there is no translation or displacement of the source. When the motorized platform is tipped or tilted, the source is stationary, while only the laser beams direction are affected.

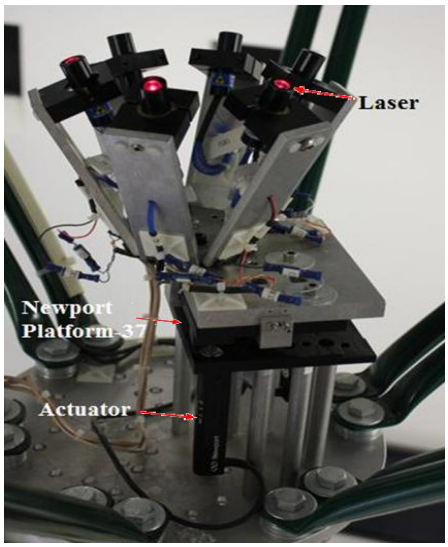

Figure 4. Laser Assembly

Using the distance from the platform's rotation point to each actuator, (a_x and a_y for the actuator on each respective axis), and the actuator displacement, it is calculated that the platform moves an angle θ from its zero position on the y-axis. The platform's normal vector also moves the same angle θ from the positive z-axis.

IV. Modal Analysis

In mathematical terms, the PPA is described by a set of equations of motion of the form:

$$M\ddot{\delta} + C\dot{\delta} + K\delta = F \tag{1}$$

where δ represents the degrees of freedom (DOF) and M, C, and K represent the global mass, internal damping, and stiffness matrices respectively, and F represents the input force (or moments) to the system. For the purpose of modeling a very rigid structure like the PPA, the internal damping is excluded (assumed to be very near 0), resulting in a first approximation of the system dynamics, (2).

$$M\ddot{\delta} + K\delta = F \tag{2}$$

With (2) in hand, the model's eigenvalues/frequencies and modeshapes (eigenvectors) can be extracted by first solving the eigenvalue problem as stated (3), obtained by setting the input force F to zero.

$$\ddot{\delta} = -M^{-1}K\delta \tag{3}$$

The eigenvectors of (3) represent the modeshapes of the system which can be compiled together to form a modal matrix, Φ, used to transform (2) into generalized coordinates, q, according to the substitution made in (4). The resulting equation of motion in terms of q is given in (5). To simplify analysis, the mass matrix M can be normalized with respect to the modal matrix (equation 6). Therefore, premultiplying (5) by the transpose of Φ, results in a simplified equation of motion in terms of q in (7).

$$\delta = Mq \tag{4}$$

$$M\Phi\ddot{q} + K\Phi q = F \tag{5}$$

$$\Phi^T M\Phi = I \tag{6}$$

$$\ddot{q} + \Lambda q = \Phi^T F \tag{7}$$

$$\Lambda = \Phi^T K\Phi \tag{8}$$

where Λ, seen in (8), is the system spectral matrix consisting of the eigenvalues of the system.

The simplified representation in (7) allows for the derivation of a mathematical model that can be used to simulate the dynamics of the PPA in software and the straight-forward derivation of a state-space model for the development of a controller. In order to identify all the DOF of interest of the physical model, first a mechanical model is developed in software, which is then meshed and used for finite element analysis (FEA) in solving (3) for the system eigenvalues and modeshapes.

V. Finite Element Model Development

Development of the PPA finite element model started with defining the PPA structure geometry in SolidWorks and saving the model as a parasolid file. The SolidWorks parasolid file is then imported to FEMAP where the material and properties are defined. Mesh analysis is performed on the model and a finite element model is constructed. This finite element model is then imported to NX NASTRAN for post processing. Normal mode analysis is performed on the model and the NX NASTRAN software outputs the mass matrix, stiffness matrix, degrees of freedom, eigenvalues, natural frequencies and mode shapes of the PPA structure in the form of text files. The procedure is shown below in Figure 5.

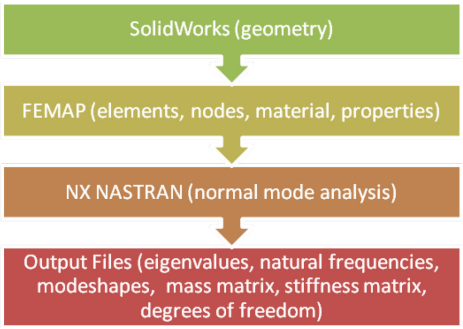

Figure 5. Finite-Element Model and Analysis Flowchart

A. SolidWorks Model

A geometric model of the PPA was developed using SolidWorks. The PPA structure was broken down and

modeled as separate parts being the six lasers, six laser holders, hexagonal plate, top platform, Newport 37 platform, two Newport linear actuators, and nine supporting rods. These parts where assembled together as shown in Figure 6 with the laser holders placed in such a way that the lasers are placed 22.84° from the platform normal (positive z-axis). The placements of the lasers were determined through a Raytracing algorithm, described in [4]. This algorithm determined the optimal location of the source relative to the SPACE Testbed by tracing the beam through vector transformations starting with the Testbed optical detectors back to where the source originated, Figure 2. Placing the lasers at this angle allows for all six lasers to originate from the same point at the platform. The units of measurement used for the model are in millimeters.

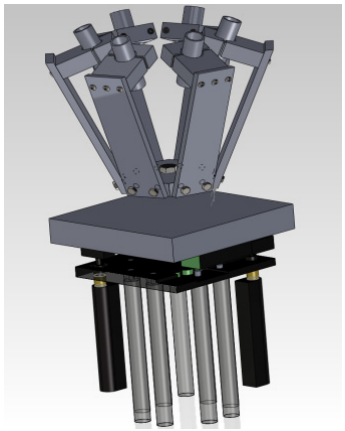

Figure 6. SolidWorks Model

The PPA is composed of two main parts which consist of a controllable and a fixed part. The controllable part is the top half section of the structure where the actuators push upwards in a linear fashion and where the Newport 37 platform has its gimbal point. The fixed part is the bottom half of the structure where the actuators, supporting rods and bottom portion of the Newport 37 platform are located. For simplicity and ease of computation the fixed part of the PPA structure was removed resulting in Figure 7. The designed geometry is saved as a parasolid file and imported into Finite Element Modeling and Post Processing (FEMAP).

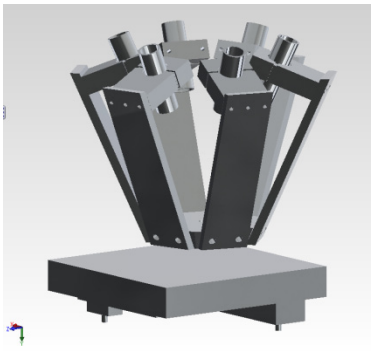

Figure 7. Updated Solidworks Model

B. FEMAP Model

The parasolid model developed in SolidWorks is imported into FEMAP for defining of the elements and properties of the PPA structure and finally performing a mesh analysis. The properties where specified to be 6061 Aluminum for the entire structure and is constructed with plate elements for simplicity of design and minimal number of elements and nodes. Mesh analysis is performed on the model resulting with 8819 nodes and 7998 elements. The element growth ratio and mesh density have to be increased using FEMAP's meshing toolbox in order to minimize the number of nodes and elements in the model but a problem arises which affects the accuracy of the results by changing these parameters. Therefore careful selection is placed on which areas of the model would be affected by the increase in element growth ratio and/or mesh density. The element growth ratio is increased throughout the model and the mesh density is increased mostly on the platform and by a small amount on the laser holders. The reason being that the platform has more mass and is more rigid than the laser holders. The minimum number of nodes and elements achieved with keeping reasonably accurate results is 5795 nodes and 4993 elements as shown in figure 8.

Constraints are to be applied to finalize the finite element model of the PPA structure. The lasers on the PPA are positioned to have the laser source originate at the rotation point of the platform. The platform is assembled with two linear actuators that provide two axis of tilt. The gimbal point is composed with hardened and polished steel ball pivots giving the gimbal point three axis angular degrees of freedom. Therefore the PPA model is constrained at three points. Two points being for the linear actuator translation are constrained in the x, y axis for translation and in the x,y,z axis for rotation. The gimbal point has a pinned constraint meaning that it is constrained in the x,y,z axis for translation. This completes the finite element modeling for the PPA structure shown in Figure 8.

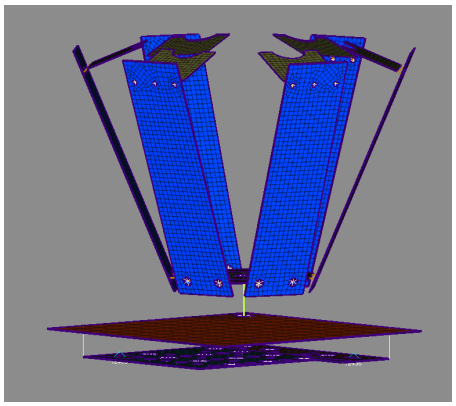

Figure 8. Finite Element Model

VI. RESULTS

By performing modal analysis, the modeshapes and their respective frequencies are obtained showing that the PPA is

a rigid structure. NX NASTRAN outputs a .f06 text file containing the natural frequencies, mode shapes, degrees of freedom, eigenvalues, and other information of the structure. The text file is filtered out and only the useful information which are the modal matrix, eigenvectors, and degree of freedom mapping are extracted as shown in figure 9.

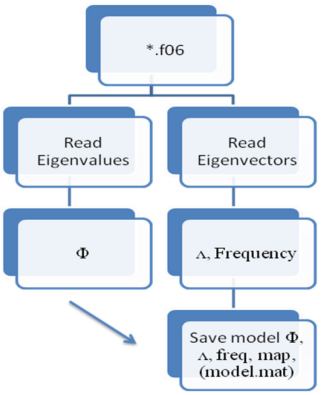

Figure 9. NX NASTRAN Output File

An initial analysis shows the frequency range for the first 100 modes ranged from 56.7 Hz to 13.017 kHz as shown in figure 10. A second analysis yields similar results, but are truncated to 20 modes (approximately 1 kHz), to reduce the size of the final state-space model and because it is determined that higher frequencies would not be of concern.

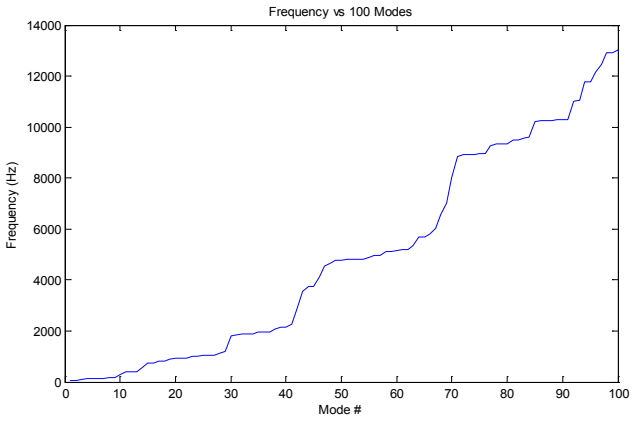

Figure 10. Frequency of first 100 modes

The first group of mode shapes corresponds to the deformations of the laser holders followed by the deformation of the platform. The deformations of mode 4 at 126.2326 Hz and mode 10 at 261.7744 Hz are shown in figure 11 and figure 12 respectively. These figures show how the laser holders are deformed at the first group of frequencies followed by the more rigid platform at higher frequencies.

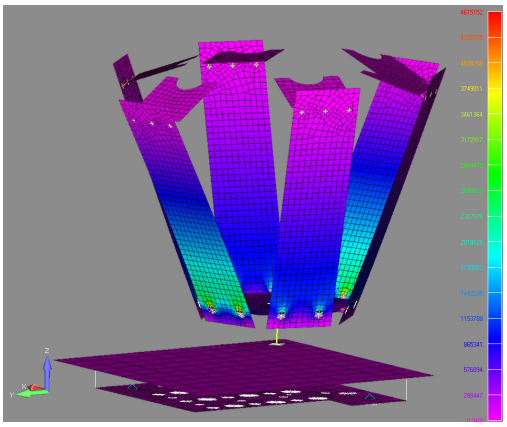

Figure 11. Mode 4, 126.2326 Hz

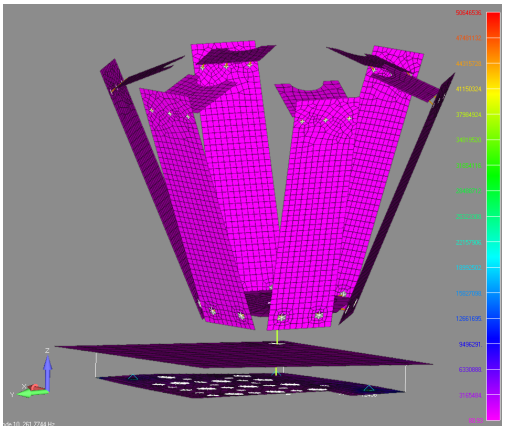

Figure 12. Mode 10, 261.7744 Hz

VII. Conclusion

In this paper a finite element model of an actuated laser platform used for a space telescope pointing control is developed. Modal analysis is performed on the finite element model which calculates the natural frequencies, mode shapes, degrees of freedom, and eigenvalues of the structure. Further research is to be undertaken to define which nodes are desirable and which nodes are unnecessary in order to be able to perform Guyan Reduction and eventually a state space representation of the PPA.

Acknowledgment

Special thanks go to the faculty and students associated with the SPACE Laboratory at California State University, Los Angeles and lab members for their contributions to this work.

References

[1] M. J. Morales, "Design and modeling of the SPACE Tesbted," M.S. Thesis, Department of Electrical Engineering, California State University, Los Angeles, Los Angeles, CA, USA, 2001.

[2] H. Boussalis, Z. Wei, and M. Mirmirani, "Dynamic Performance Modeling and Decentralization of A Segmented Reflector Telescope," IASTED Conference on Modeling and Simulation, Mexico, 1995.

[3] H. Boussalis, "Decentralization of Large Spaceborne Telescopes", Proc. 1994 SPIE Symposium on Astronomical Telescopes, Hawaii, 1994.

[4] A. Desai, J. Alvarenga, H. Tarsaria, K. Rad, H. Boussalis, “Ray Tracing Visualization Using LabVIEW for Precision Pointing Architecture of a Segmented Reflector Testbed,” MED 2011, Corfu, Greece, June 2011.
[5] H. Boussalis, M. Mirmirani, A. Chassiakos, K. Rad, “The Use of Decentralized Control in Design of a Large Segmented Space Reflector”, Control and Structures Research Laboratory, California State University, Los Angeles, Final Report, 1996.
[6] H. Boussalis, K. Rad, A. Khosafian, Y. Komandyan, “Pointing Control Testbed for Segmented Reflectors”, June 2005.
[7] H. Boussalis, “Stability of Large Scale Systems”, New Mexico, USA, November, 1979.
[8] Helen Boussalis, “The Use of Decentralized Control in Design Of A Large Segmented Space Reflector”, Structure Pointing and Control Laboratory, California State University, Los Angeles, Final Technical Report, 2002.
[9] K.J. Bathe, and E.L. Wilson, Numerical Methods in Finite Element Analysis, 2nd Ed., John Wiley and Sons, 1976.
[10] C.H. Ih, H.C. Briggs, S.J. Wang, “3D Dynamic Modeling and Simulation of a Precision Segmented Reflector Telescope”, Proceedings of the 21st Annual Pittsburgh Conference, 1990.
[11] H. Ryaciotaki-Boussalis, H.C. Briggs, and C.H. Ih, “Dynamic Performance Modeling and Stability Analysis of a Segmented Reflector Telescope,” Proceedings of the 1991 Automatic Control Conference, pp. 1705-1706, 1991.
[12] Carrier, A.C., “Modeling and Shape control of a Segmented-Mirror Telescope,” Ph.D. dissertation, Dept. Aeronautics and Astronautics, Stanford Univ., Stanford, CA, 1990.
[13] R.D. Cook, Concepts and Applications in Finite Element Analysis, 2nd Ed., John Wiley and Sons, 1981.
[14] R. Bishop, and D.C. Johnson, The Mechanics of Vibration, Cambridge University Press, 1981